Received: 13 February 2022 | Revised: 18 November 2022 | Accepted: 17 December 2022

DOI: 10.5185/amlett.2023.031727

RESEARCH

Effects of Initial Surface Roughness and Sliding Speed Study on the Tribological Characteristics of AA6061 and CuZn37Pb2 Alloys

Bougoffa M. Seyf Eddine[1,*] | Sayhia Benchaa[2]

[1]Laboratory of Materials Technology, Department of Materials Science, Université de Science et de Technologie Houari Boumediene (USTHB), Bp 32 El Alia 16111 Bab Ezzouar, Algiers, Algeria

[2]Laboratoire de Rayonnement et Plasmas et Physique des Surfaces (LRPPS), Faculté des Mathématiques et des Sciences de la Matière, Université de Ouargla, 30000 Ouargla, Algeria

***Corresponding author:**
E-mail: mbougoffa@usthb.dz

ABSTRACT

The paper examines the influence of initial surface roughness and sliding speed on friction and wear behavior of AA6061 aluminum alloy and brass alloy (CuZn37Pb2) under dry contact using a CSM tribometer. Surface roughness of materials studied were measured using optical profilometer. Rough surfaces (Ra=0.37 - 1.33 µm) were prepared on two materials: AA6061 and CuZn37Pb2 alloy. Track width, wear rate, and wear loss values were assessed and contrasted with changes in coefficient of friction values at various starting surface roughness and sliding speeds. Experiments are conducted at sliding speed 0.15;0.24;0.35 and 0.48 m/s. wear track diameter 4;6;8;10 mm. Results show that wear loss, wear rate and track width of CuZn37Pb2 and AA6061 increase at high initial surface roughness and speed but the value of friction coefficient decreases. Various SEM analysis of the wear trace and worn surfaces for each alloy at different sliding speed were analysed and compared.

KEYWORDS

Initial surface roughness, sliding speed, friction coefficient, wear loss, wear rate.

INTRODUCTION

The researched alloys, CuZn37Pb2 and AA6061, are frequently employed in applications requiring excellent wear resistance. It is well known that the tribological behavior of the materials in contact depends on a number of interrelated tribological characteristics [**1-8**]. The tribological behavior of alloys and materials needs to be understood and predicted in order to be used in modern industrial applications. It's important to research the effects of the various factors that affect friction and wear behavior, including normal force and speed. Numerous tests have been carried out [**9-17**] to learn more about the characteristics of AA6061 and CuZn37Pb2. Amid relative movement of two surfaces, different kinds of wear mechanisms, including adhesion wear, fatigue wear, delimitation wear, abrasion wear, erosive wear, and destructive/oxidative wear have been significantly reported [**14-16**]. According to Liu *et al.* [**17**], the wear volume and load for laser-prepared Al- Gr composites with 1.55 wt% Gr are directly correlated. For the prediction of the material flow and temperature distribution on the specimen at the ring upsetting, see Nagpal *et al.* [**18**]. Li *et al.* [**19**] have examined the effects of lubricant on friction coefficients according to temperature. Mahrenholtz *et al.* investigated how roughness affected several 3D models and demonstrated the impact of asperity density distribution on the normal compliance law [**20**].

However, as wear is an evolutionary and irreversible event, the tribological behavior of these materials is not well understood, which makes our investigation in the laboratory rather unique. There are numerous ways to test for sliding wear [**21**]. The films present at the contact play a role in the tribological behavior of the alloy pairs [**22**].

This study suggests examining the friction and wear behavior of CuZn37Pb2 and AA6061 in this setting. These alloys have good tribological properties, including resistance to oxidation and wear. The information pertaining to the changes in the metallographic structure happening on the surface and volume, when these two materials have a distinct microstructure but are machined with a similar level of roughness and hardness, is yet unknown. We have hurdles in filling this knowledge gap. This study helps to establish the first cornerstone for connecting academic knowledge to practical experience in the workplace.

In order to improve performance and quality in industry, this study aims to assess the dry sliding wear behavior of AA6061 and CuZn37Pb2 by performing pin-on-disc tests with varying loads, speeds, and roughness.

EXPERIMENTAL PROCESS

Trial device and materials

Tests for dry sliding wear were performed on a tribometer made by CSM. CuZn37Pb2 and AA6061 were utilized as the disc. While the ball was made of 100Cr6 martensitic steel (52100). For situations where excellent mechanical performance is sought, martensitic stainless steels are typically used [**23-25**]. The samples were polished with 240, 600, and 1200-grit silicon carbide sheets to provide the desired characteristics and surface finish, while the balls were used in their soft, as-received form.

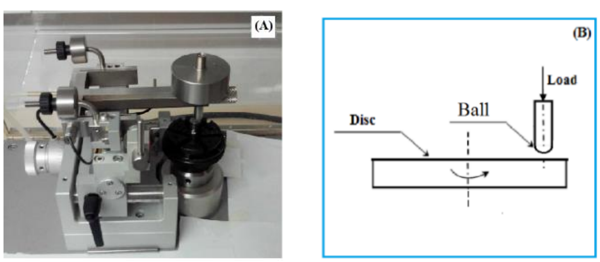

Fig. 1. (A) View of the CSM Tribometer and (B) pin-on-disc configuration

As a disc, CuZn37Pb2 and AA6061 are employed. While the ball was made of 100Cr6 martensitic steel (52100). For situations where excellent mechanical performance is sought, martensitic stainless steels are typically used [**22-24**]. **Table 1** displays the information.

Table 1. Summary of materials tested

Type	Alloys	Hardness	Surface Roughness Ra[µm]
Samples	AA6061 aluminum alloy	150±0.5 HB	0.48-0.76- 1.33
	brass (CuZn37Pb2)	63.2±0.5 HRB	0.37-0.62- 1.24
Ball	AISI 52100 steel	780 HV30	0.09±0.003

Experimental procedure

Wear loss of the CuZn37Pb2 and AA6061 sample are considered as a wear parameter evolving in function of time. The wear rate were calculated using the expressions [**26,27**]. The detail experimental conditions are shown in **Table 2**.

Table 2. Summary of the pin-on-disc test parameters.

N °	Parameters	Unit	Value(s)
1	Normal load	N	3 - 5 – 8 - 10
2	Sliding speed	m/s	0.15 - 0.24 - 0.35 – 0.48

RESULTS AND DISCUSSION

In both research and practical applications, initial surface roughness in dry conditions is frequently disregarded. There is a dearth of literature on early surface roughness in friction and wear. The coefficient of friction found in this investigation generally agrees to some extent with other findings [**19**]. In this study, the effects of surface roughness and sliding speed on tribological properties of AA6061 and CuZn37Pb2 are discussed. Wear loss and track width have been associated with variations in the coefficient of friction in dry sliding wear at various beginning surface roughness and sliding speed. Experiments are carried out with wear track diameters of 4-6-8-10 mm at sliding speeds of 0.15-0.24-0.35 and 0.48 m/s.

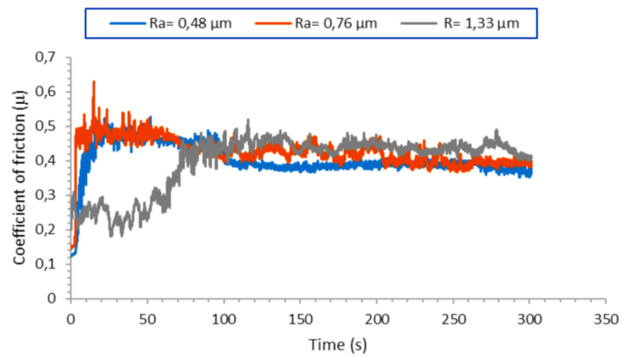

Fig. 2. COF of AA6061 with time at different initial surface roughness.

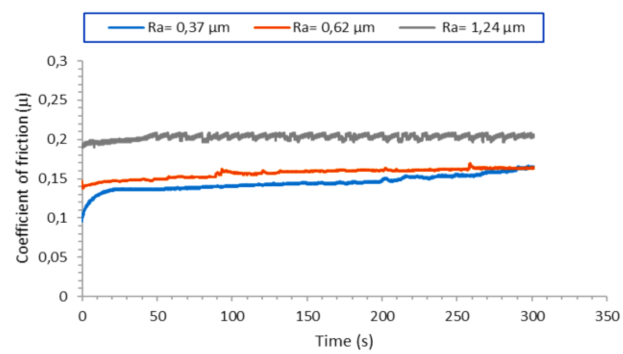

Fig. 3. COF of CuZn37Pb2 with time at different initial surface roughness.

Friction analysis

Fig. 2 and **Fig. 3** depict how the initial surface roughness of the materials AA6061 and CuZn37Pb2 has an impact on how the average friction coefficient changes over time. As a result of the initial roughness of the sample, the friction for AA6061 is unstable, according to the data. The impact of the initial surface roughness is more for CuZn37Pb2. And see **Fig. 2** for that. **Fig. 3** shows that the value of surface roughness (Ra) = 1,33 m for AA6061 yielded the highest value of coefficient of friction (0.40), whereas the value of surface roughness (Ra) = 1,24 m for CuZn37Pb2 yielded the highest value of coefficient of friction (0.21). These numbers indicate that the friction coefficient is increased by surface roughness. The findings of this research are compatible with the observation of other researchers [**20,21**].

Fig. 4 and **Fig. 5** depict the evolution of the coefficient of friction between CuZn37Pb2 and AA6061 under various normal loads and a constant 35 m/s sliding speed. The evolution of the friction coefficients of AA6061 and CuZn37Pb2 under various conditions of sliding speed, initial surface roughness, and constant normal load (5N) is shown in **Fig. 6** and **Fig. 7**. These numbers show that when normal load and sliding speed rise, the friction coefficient lowers. The method by which the pin is transferred to the disc is primarily responsible for this. In fact, surfaces cling to one another at low stresses due to the antagonists' imbrication (tangle) asperities, boosting the adhesion of the surfaces in contact. With an increase in sliding speed and normal load, the friction coefficient of the materials AA6061 and CuZn37Pb2 decreased. This can be due to a change in the shear rate, which could affect the mechanical and tribological properties of the materials in contact. These materials' strength improves with increasing shear strain rates [**22**], which reduces the real area of contact and the coefficient of friction during dry sliding.

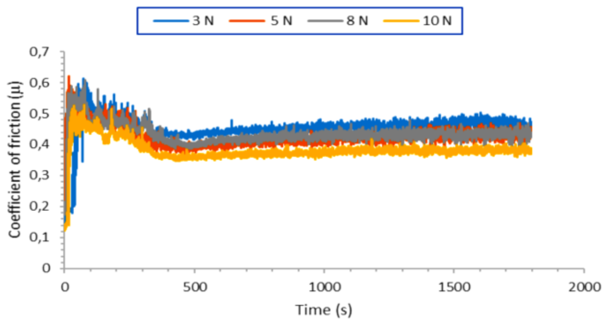

Fig. 4. Coefficient of friction of AA6061 with time at different normal load.

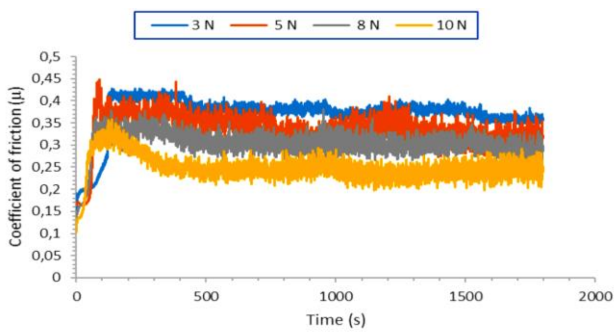

Fig. 5. Coefficient of friction of CuZn37Pb2 with time at different normal load.

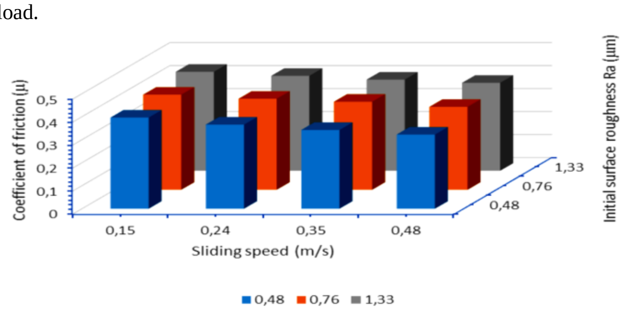

Fig. 6. Friction coefficient values of AA6061 with different sliding speed and initial surface roughness.

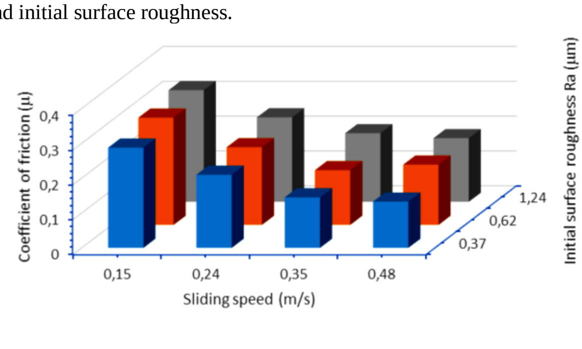

Fig. 7. Friction coefficient value of CuZn37Pb2 with sliding speed and initial surface roughness.

Fig. 8 displays the coefficient of friction for AA6061 and CuZn37Pb2 during dry sliding wear at various sliding speeds. experiment carried out at a wear track diameter of 6 mm. According to the findings, the friction coefficient for AA6061 and CuZn37Pb2 decreases from 0.49 at 0.15 m/s to 0.42 at 0.48 m/s and from 0.40 at 0.15 m/s to 0.28 at 0.48 m/s, respectively. It is obvious that CuZn37Pb2 exhibits significantly lower friction than AA6061 under the same circumstances.

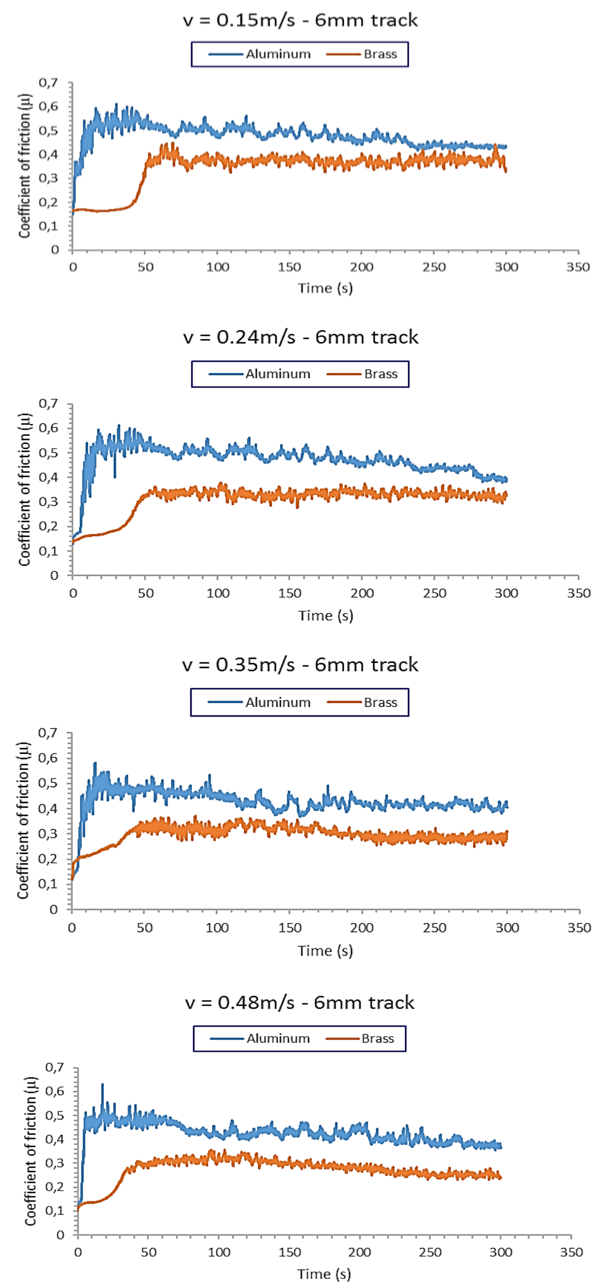

Fig. 8. Friction coefficient curves of CuZn37Pb2 and AA6061 for: different sliding speed, tests conducted at 6 mm wear track.

Fig. 9 and **Fig. 10** show the view of samples after wear test, visibly it can see the traces of wear with different diameters, we conclude that the studied material does not show the same tribological response.

Fig. 9. View of AA6061 after wear test

Fig. 10. View of CuZn37Pb2 after wear test

Fig. 11 displays the coefficient of friction measured during dry sliding wear of CuZn37Pb2 and AA6061 at various wear track sizes. The outcomes supported the theory that friction and wear on the surface can be consistently produced by the strategy of using concentric wear tracks of various diameters [**23**]. It has been demonstrated that the coefficient of friction curves hardly alter and that the diameters of the track wear have no discernible relationship to the coefficient of friction's variation.

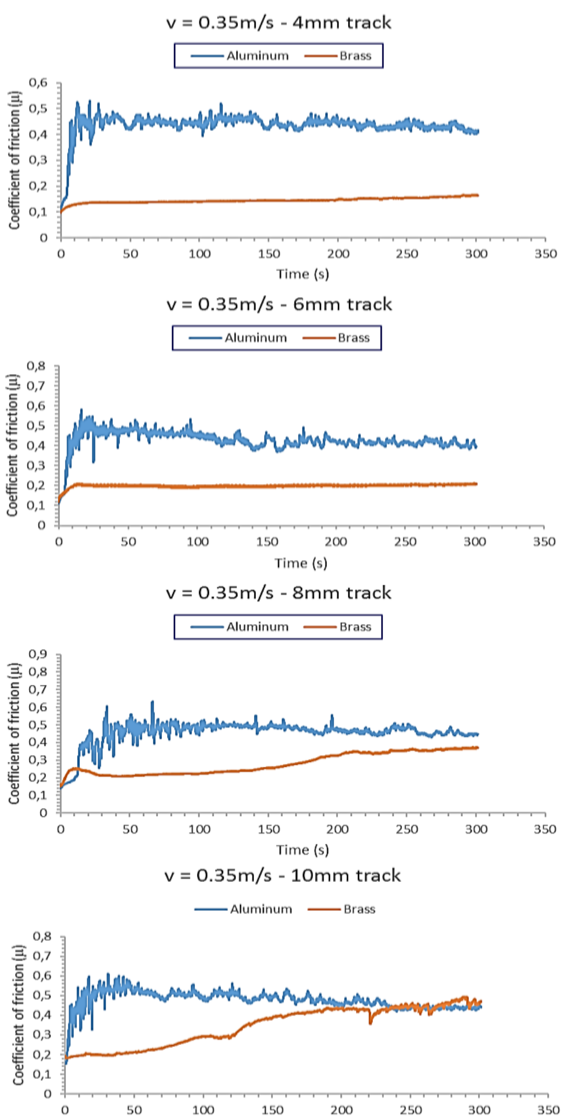

Fig. 11. Friction coefficient curves of CuZn37Pb2 and AA6061 for load: 5N, tests conducted at different wear track diameters.

Fig. 12 and **Fig. 13** show the view of samples (CuZn37Pb2 and AA6061) after wear test, visibly it can see the traces of wear with different diameters, we conclude that the studied material does not show the same tribological response.

Fig. 12. View of AA6061 after wear test

Fig. 13. View of CuZn37Pb2 after wear test

Wear analysis

The graphs (**Fig. 14** and **Fig. 15**) display the wear loss values for CuZn37Pb2 and AA6061 at various speeds and roughness levels. The findings demonstrate that for two alloys, wear loss rises at high sliding speeds and high start surface roughness values, whereas it falls at low sliding speeds and low initial surface roughness values. For AA6061, a sliding speed of 0.48 m/s and an initial surface roughness of 1.33 m produce the higher wear loss. For CuZn37Pb2, a sliding speed of 0.48 m/s and an initial surface roughness of 1.24 m yield the higher wear loss. The outcomes are mostly in line with what the authors discovered [**17,18**].

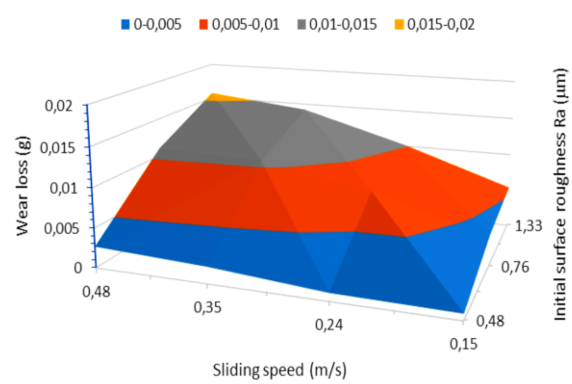

Fig. 14. Surface plot for wear loss of AA6061 versus sliding speed and initial surface roughness

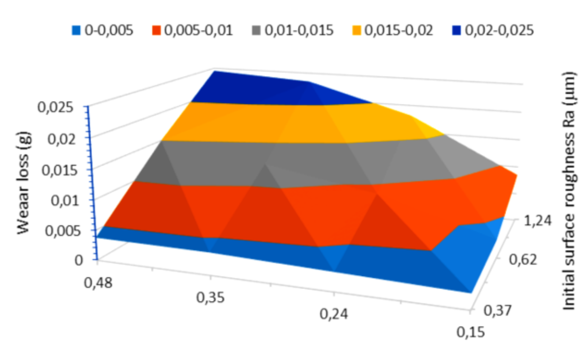

Fig. 15. Surface plot for wear loss of CuZn37Pb2 versus sliding speed and initial surface roughness.

Plots of the wear rates of CuZn37Pb2 and AA6061 at various initial surface roughness and sliding speed are shown in **Fig. 16** and **Fig. 17**. According to the findings, wear rates for two alloys increase at high beginning surface roughness and drop at high sliding speeds, whereas wear rates increase at low sliding speeds and reduce at low starting surface roughness values. For AA6061, a sliding speed of 0.15 m/s and an initial surface roughness of 1.33 m yield the greater wear rate. For CuZn37Pb2, a sliding speed of 0.15 m/s and an initial surface roughness of 1.24 m yield the greater wear rate.

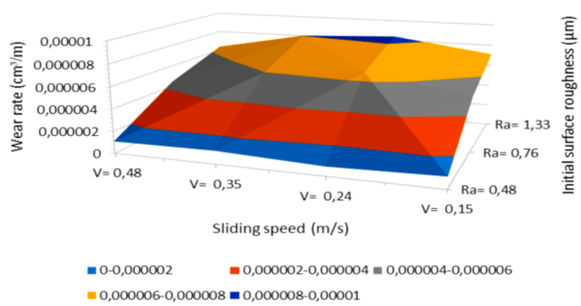

Fig. 16. Surface plot for wear loss of AA6061 versus sliding speed and initial surface roughness

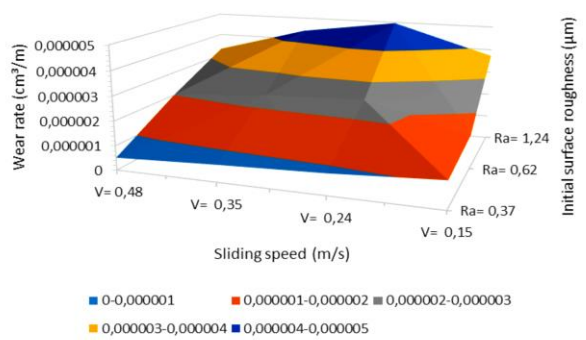

Fig. 17. Surface plot for wear loss of CuZn37Pb2 versus sliding speed and initial surface roughness

The effects of normal load and sliding speed on the coefficient of friction, wear loss, and track width of AA6061 and CuZn37Pb2 are depicted in **Fig. 18** to **Fig. 21**. These statistics show that the track width, wear loss, and coefficient of friction are all influenced by the load being applied and the sliding speed. According to the findings, the track width increases with wear loss when the usual load or sliding speed increases, yet the coefficient of friction decreases. The findings are remarkably in line with what has been discovered through study [**19,20**].

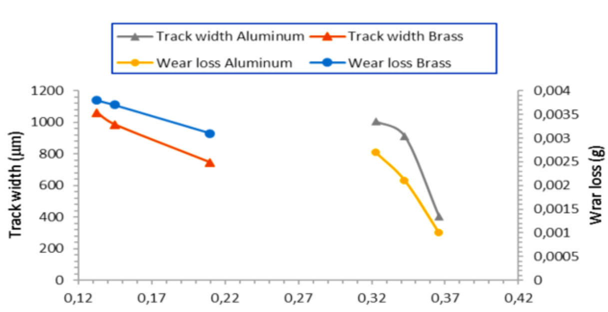

Fig. 18. Track width and wear loss of AA6061 and CuZn37Pb2 with the variation of coefficient of friction at different normal load and sliding speed.

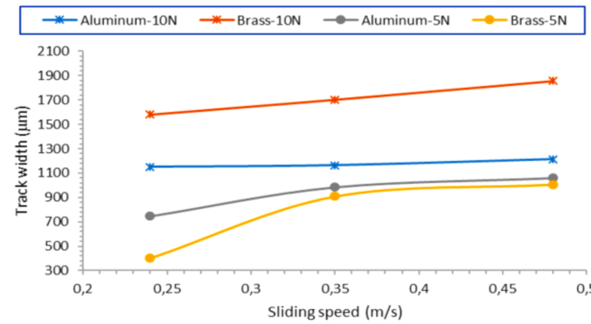

Fig. 19. Variation of track width of AA6061 and CuZn37Pb2 with different load and sliding speed

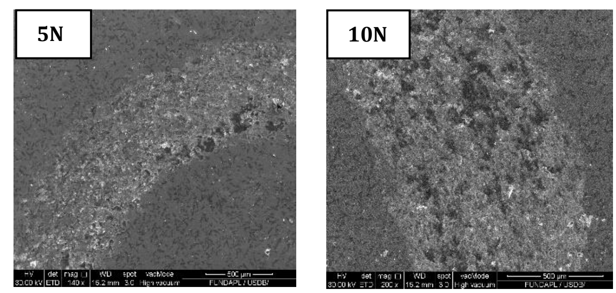

Fig. 20. SEM micrographs track width surface of AA6061 at different normal load.

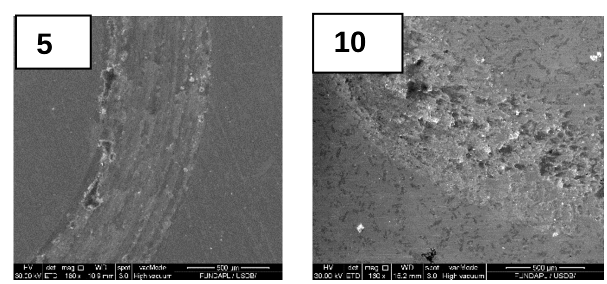

Fig. 21. SEM micrographs track width surface of CuZn37Pb2 at different normal load.

Worn surface analysis

Fig. 22 depicts the surface morphology of CuZn37Pb2 and AA6061 after various sliding speeds. **Fig. 22** for CuZn37Pb2 (A) and AA6061 (D) shows that under a modest sliding speed of 0.24 m/s, there were clear cut lines and grooves on the worn surface as well as a flake stripping layer in the local structure. This suggests that abrasive wear, a little spalling wear, and some wear debris with an abrasive action are the main types of wear that occur under such sliding speeds. Wear debris specifically its chemical makeup is what causes the presence of oxides. Studies have revealed that when debris oxidizes during contact, the friction coefficient increases noticeably. Spinler [**27**] was aware that the coefficient of friction increases significantly when the contact surfaces are degraded and that it is often high when surfaces are quite rough. The range of the spalling area also expanded as the sliding speed increased, increasing the width and depth of the grooves. Figure 22 for CuZn37Pb2 (C) and AA6061 illustrates the extreme plastic deformation of the wear surface at 0.48 m/s sliding speed (F). The quantity and scope of plastic deformation and material peeling will therefore rise with an increase in sliding speed, resulting in roughened wear surfaces and significant wear loss.

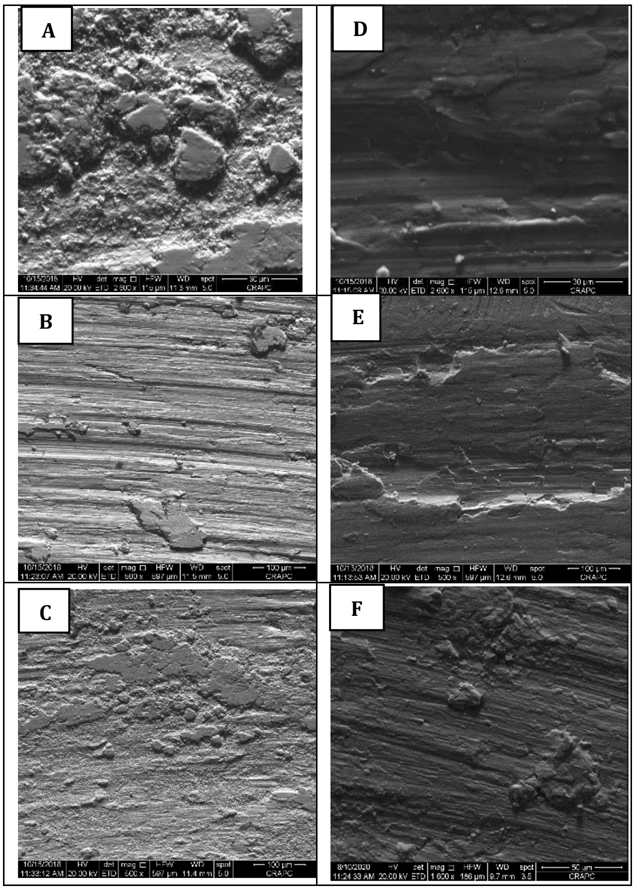

(A)0.24 m/s; (B) 0.35 m/s; (C) 0.48 m/s; CuZn37Pb2 for 5N
(D) 0.24 m/s; (E) 0.35 m/s; (F) 0.48 m/s; AA6061 for 5N

Fig. 22. SEM micrographs of CuZn37Pb2 and AA6061 at different loads and sliding speeds

CONCLUSION

The objective of this study is to assess and compare the effects of starting surface roughness and sliding speed on the tribological properties of the alloys CuZn37Pb2 and AA6061 when sliding in dry conditions. The outcomes support the following findings:

For CuZn37Pb2 as opposed to AA6061, the effect of initial surface roughness on the coefficient of friction is more significant. Wear loss is accelerated by an increase in frictional thrust and shear force brought on by a rise in sliding speed. The test showed unequivocally that the initial surface roughness correlates with the transition stress and wear rate in going from high to low wear. When AA6061 and CuZn37Pb2 come into contact with each other under conditions of positive load and speed, there is a significant correlation between the coefficient of friction, wear loss, and track width.

The conclusion of this study suggests that studies of friction and corrosion behavior should be given more consideration in the future, and they should be singled out for numerous experimental investigations in order to gather more data and provide answers to numerous open-ended questions.

ACKNOWLEDGEMENTS

The authors would like to acknowledge: Scientific Research Center of Physico-Chemical Analysis (CRAPC).

AUTHOR'S CONTRIBUTIONS

Authors have no competing financial interests.

REFERENCES

1. Katoch, Sanjeev; Sehgal, Rakesh; Singh, Vishal; Wear behavior of differently cryogenically treated AISI H13 steel against cold work steel, *Proc I Mech E Part E*: J Process Mechanical Engineering, Singh first published online: June 9, **2018**.
2. Matlin, M.M.; Kazankina, E.N.; Kazankin, V.A.; Effect of Ratio of Hardnesses, Load, and Roughness Parameters on Approach in Elastoplastic Contact of Rough Surfaces of Flat Parts, *Journal of Friction and Wear*, **2016**, *37, 4,* 320-323.
3. Coronado, J. J.; Abrasive Size Effect on Friction Coefficient of AISI 1045 Steel and 6061-T6 Aluminium Alloy in Two-Body Abrasive Wear, *Tribol Lett* (**2015**) *60:40*.
4. Lang, Andrej; Klüppel, Manfred; Influences of temperature and load on the dry friction behaviour of tire tread compounds in contact with rough granite, *Wear*, **2017**, *380-381*, 15-25.
5. Yi, Yanliang; et al, Effect of normal load on two-body abrasive wear of an Fe-B-Cr-C based alloy with minor Cu and Ni additions, *Wear*, **2018**, *408-409*, 160-170.
6. Mishakin, V.V.; Verichev, S.N.; Razov, E.N.; Investigation of the Influence of High Hydrostatic Pressure on the Abrasive Wear of Hard-Alloy Materials, *Journal of Friction and Wear*, **2017**, *38,* 4, 286-291.
7. Kolesnikov, V.I.; Zarif'yan, A.A.; Sychev, A.P.; Kolesnikov, I.V.; The Effect of the Coefficient of Journal Friction in Ball-and-Socket Bogie Body Pivots on the Work Done by Friction Forces in Curvilinear Motion, *Journal of Friction and Wear*, **2016**, *37,* 5, 476-481.
8. Elhadi, A.; et al, Study of Surface Wear and Damage Induced by Dry Sliding of Tempered AISI 4140 Steel against Hardened AISI 1055 Steel, *Tribology in Industry*, **2016**, *38*,4, 475-485.
9. Zambelli, G. ; Vincent, L. ; Matériaux et contacts, une approche tribologique, Presse polytechniques et universitaires romandes, Suisse, **1998**.
10. Da Hai, H.; Rafael, M.; A novel electrical contact material with improved self-lubrication for railway current collectors, *Wear,* **2001**, *249,* 626-636.
11. Ma, X.P.; Wang, L.J.; Liu, C.M.; Subramanian, S.V.; Microstructure and properties of 13 Cr 5 Ni 1 Mo 0.025 Nb 0.09 V 0.06 N super martensitic stainless steel. *Mater. Sci. Eng., A,* **2012**, *539,* 271-279.
12. Thibault, D.; Bocher, P.; Thomas, M.; Residual stress and microstructure in welds of 13%Cr– 4%Ni martensitic stainless steel. *J. Mater. Process. Technol*., **2009**, *209,* 2195-2202.
13. Li, C.X.; Bell, T.; Corrosion properties of plasma nitrided AISI 410 martensitic stainless steel in 3.5 % NaCl and 1 % HCl aqueous solutions. *Corros. Sci.*, **2006**, *48,* 2036-2049.
14. Meng, H.C.; Ludema, K.C.; Wear models and predictive equations: their form and content. *Wear*, **1995**, *181-183*, 443-457**.**
15. Challen, J.M.; Oxley, P.L.B.; An explanation of the different regimes of friction and wear using asperity deformation models, *Wear*, **1979**, 53, 229-243.
16. Bhushan, B.; Israelachvili, J.N.; Landman, U.; Nanotribology: Friction, wear and lubrication at the atomic scale, *Nature*, **1995**, *374,* 607-616.
17. Liu, Y.B.; Hu, J.D.; Cao, Z.Y.; Rohatgi, P.K.; Wear resistance of laser processed Al–Si–graphite composites, *Wear*, **1997**, *206,* 83-86**.**
18. Nagpal, V.; Lahoti, GD.; Altan T.; A numerical method for simultaneous prediction of metal flow and temperatures in upset forging of rings. *J Eng Ind*., **1978**, 100, 413-20.
19. Li, LX; Peng, DS; Liu, JA; Liu, ZQ; Jiang, Y.; An experimental study of the lubrication behavior of A5 glass lubricant by means of the ring compression test. *J Mater Process Tech*., **2000**, *102,* 138-42.
20. Mahrenholtz, O.; Bontcheva, N.; Iankov, R.; Influence of surface roughness on friction during metal forming processes. *J. Mater. Process Tech*., **2005**, *159,* 9-16.

21. Stachowiak, G.W.; Batchelor, A.W.; Engineering Tribology, Butterworth-Heinemann, **2005**.
22. Kumar, Hemant; et al, Friction and wear behaviour of Ni-Cr-B hardface coating on 316LN stainless steel in liquid sodium at elevated temperature, *Journal of Nuclear Materials*, **2017**, 495, 431e437.
23. Rabinowicz, E.; Friction and Wear of Materials, 2nd Edition, Wiley, **1995**.
24. Okonkwo, Paul C.; Kelly b, Georgina; Bernard F. Rolfe c; Michael P. Pereira; The effect of sliding speed on the wear of steel–tool steel pairs, *Tribology International*, **2016**, *97,* 218-227.
25. Zhang, Sheng-cheng; Qing-lin PAN1,2, Jie YAN1, Xing Huang1, Effects of sliding velocity and normal load on tribological behavior of aged Al−Sn−Cu alloy, *Trans. Nonferrous Met. Soc. China*, **2016**, *26,* 1809-1819.
26. Okonkwo PC; et al. The effect of temperature on sliding wear of steel-tool steel pairs. *Wear,* **2012**, *282-283,* 22-30.
27. Spinler, G.; Machine Design, Principles and Applications, 1 Static, 2nd Ed. EPFL Press and Chapman & Hall: Lausanne, **2002**.